

BB

**MICHIGAN STATE  
UNIVERSITY**

**National Superconducting Cyclotron Laboratory**

**EVIDENCE FOR AN  $l = 0$  GROUND STATE IN  ${}^9\text{He}$**

**L. CHEN, B. BLANK, B.A. BROWN, M. CHARTIER,  
A. GALONSKY, P.G. HANSEN, M. THOENNESSEN**

CERN LIBRARIES, GENEVA



CM-P00042694



**NSCL**

**MSUCL-1193**

**MARCH 2001**

# Evidence for an $l=0$ Ground State in ${}^9\text{He}$

L. Chen <sup>a,b</sup> B. Blank <sup>a,1</sup> B. A. Brown <sup>a,b</sup> M. Chartier <sup>a,c,1</sup>  
A. Galonsky <sup>a,b</sup> P. G. Hansen <sup>a,b</sup> M. Thoennessen <sup>a,b,\*</sup>

<sup>a</sup>*National Superconducting Cyclotron Laboratory, East Lansing, Michigan  
48824-1321, USA*

<sup>b</sup>*Department of Physics & Astronomy, Michigan State University, East Lansing,  
Michigan 48824-1321, USA*

<sup>c</sup>*Oak Ridge National Laboratory, P. O. Box 2008, Oak Ridge, TN 37831-6368,  
USA*

---

## Abstract

The unbound nuclear systems  ${}^{10}\text{Li}$  and  ${}^9\text{He}$  were produced in direct reactions of 28 MeV/u  ${}^{11}\text{Be}$  incident on a  ${}^9\text{Be}$  target. The distributions of the observed velocity differences between the neutron and the charged fragment show a strong influence of final-state interactions. Since the neutron originates in a dominant  $l=0$  initial state, a selection-rule argument allows a firm  $l=0$  assignment for the lowest odd-neutron state in  ${}^{10}\text{Li}$ . We report the results suggesting a very similar unbound state in  ${}^9\text{He}$ , characterized by an  $s$ -wave scattering length more negative than  $-10$  fm corresponding to an energy of the virtual state of less than 0.2 MeV. Shell-model calculations cast light on the reasons for the disappearance of the magic shell gap near the drip line.

*Key words:* Stripping reactions with radioactive nuclear beams,  ${}^9\text{He}$  ground state  
*PACS:* 21.10.Dr, 25.70.Mn, 27.20.+n

---

The region of the lightest nuclei offers our only practical possibility for obtaining a glimpse of the structure of nuclear systems that are “beyond the neutron drip line”, *i.e.*, that have no states that are bound with respect to neutron emission. There is a special theoretical interest in the lightest  $N=7$  isotones where intruders from the  $1s0d$  shell appear. First known in the lightest bound  $N=7$  nucleus  ${}^{11}\text{Be}$  [1], this phenomenon provides a sensitive test of

---

\* Corresponding author.

*Email address:* thoennessen@nsc1.msu.edu (M. Thoennessen).

<sup>1</sup> Permanent address: Centre d’Etudes Nucléaires de Bordeaux-Gradignan, BP 120, Le Haut Vigneau, 33175 Gradignan Cedex, France

theories designed to bridge the  $0p - 1s0d$  shells and offers a paradigm for the disappearance of the shell gaps near the neutron drip line. A number of experiments have searched for the lowest levels in  $^{10}\text{Li}$ , see the recent summary in [2]. The picture emerging is that the  $p$ -state, which is the normal ground state for  $N=7$ , and also states with higher angular momentum are detected as relatively narrow resonances in inclusive reactions. On the other hand, these reactions seem to miss the unbound  $s$ -states, which do not exhibit a resonance-like structure, but show a rapid rise in cross section at threshold followed by a slow decay towards higher energies. A Breit-Wigner shape is never a good approximation to these. It has taken a different technique based on exclusive studies of the  $^9\text{Li}+n$  channel [2–5] at low energy to find a candidate for an  $l=0$  assignment, supported by indirect arguments. In the case of  $^9\text{He}$  [6–8], inclusive measurements identified a resonance at 1.2 MeV assumed to be the ground state. Its relatively narrow width speaks for an  $l=1$  assignment and suggested [9] that there is no level inversion in this system. In the following we describe a technique specifically chosen to be sensitive to  $s$  strength at low energies, and we report the observation of a low-lying  $l=0$  level in  $^9\text{He}$  and the confirmation of the  $l=0$  assignment to the lowest neutron state in  $^{10}\text{Li}$ .

The experiment is based on a technique that we may refer to as a direct reaction leading to continuum states, and it exploits an approximate selection rule linking the single-particle structure of the initial state to that of the final state. The ideal identification of  $l=0$  strength would, of course, be elastic neutron scattering on the appropriate radioactive targets, were it not for their short half lives, 0.1–0.8 s. As in the previous work [2–5] we observe instead the reaction channel in which a neutron and the fragment of interest are emitted together. This amounts to observing the final-state interactions and was the original method used for determining the strength of the neutron-neutron interaction [10]. It is applicable if the interaction is of short range, strong and attractive, all of which holds for our cases. However, instead of producing the exit channel in a complex breakup reaction, we have in the new experiment used direct reactions corresponding to single and double proton knockout on the projectile  $^{11}\text{Be}$ . The initial neutron state of this nuclide is dominated [1] by a  $1s_{1/2}$  single-particle orbital, and it is very difficult to access an odd-parity neutron state without a major rearrangement. On the other hand, reactions on  $^{12}\text{Be}$  with filled and partly filled  $p_{3/2}$ ,  $p_{1/2}$ ,  $d_{5/2}$ , and  $s_{1/2}$  pairs connect, as we shall show, to both even- and odd-parity final states. We may assume that the two-proton removal to  $^9\text{He}$  proceeds via a direct reaction because the large difference in  $^{11}\text{Be}$  neutron separation energy (0.5 MeV) and proton separation energy (20.6 MeV) makes an intermediate step involving proton evaporation very unlikely.

The experiment was performed with radioactive beams of the three beryllium isotopes  $^{10,11,12}\text{Be}$ , all at 30 MeV/u. They were produced in the National Superconducting Cyclotron Laboratory’s A1200 fragment separator [11] from

primary beams of 80 MeV/u  $^{13}\text{C}$  and  $^{18}\text{O}$  interacting in thick production targets, and purified by intermediate aluminum degraders. A thin, fast plastic detector in the flight path upstream of the experimental area provided an event-by-event identification of the incoming particles. The fragments reacted in a 200 mg/cm<sup>2</sup> secondary  $^9\text{Be}$  target so that the mid-target energy of the projectiles was 28 MeV/u. Charged reaction products and the unreacted secondary beam were deflected by a 1.5 Tesla sweeping magnet, which was part of the fragment detection system [12]. Particle identification of the outgoing fragments was provided by the combination of the energy loss, measured in 58.2 mg/cm<sup>2</sup> silicon-strip detectors placed behind the target, and the total energy. The latter was measured in an array of sixteen vertical plastic scintillator bars 1.7 m after the target with photomultipliers placed at either end to determine the vertical position of the charged fragment. The resulting velocity resolution obtained with an incident  $^{11}\text{Be}$  beam expressed in terms of the standard deviation  $\sigma_f$  becomes 0.08 and 0.13 cm/ns for  $^9\text{Li}$  and  $^8\text{He}$ , respectively. The neutrons were detected in the two  $2 \times 2$  m<sup>2</sup> NSCL Neutron Walls [13] centered around  $0^\circ$ . The two walls were 5.0 and 5.5 m behind the target position. The resolution  $\sigma_n$  on the neutron velocity was 0.24 cm/ns independent of the reaction. The analysis included events inside a maximum angle between projectile residue and neutron of  $5^\circ$  for the  $^{10}\text{Li}$  experiment and  $10^\circ$  for the  $^9\text{He}$  experiment. This selection was taken into account in the theoretical distributions presented below. The acceptance drops rapidly for decay energies greater than 0.5 MeV. Further details of the experimental setup and analysis are published elsewhere [13–15]. It is convenient to present the results in terms of the scalar velocity difference between the almost parallel neutron and fragment [2,3]. As long as the angle between the two is small, this difference is identical to the projection of the velocity difference on the direction of the outgoing fragment.

The analysis is based on the sudden approximation. The outcome of the reaction is then obtained by expanding the initial state (a neutron bound to the rest of the projectile) in continuum eigenfunctions representing outgoing waves of the (in principle unknown) final system. Since the initial state does not belong to the same function space as the final states, there is no orthogonality requirement. The single-particle wave functions, both initial and final, were calculated for a Woods-Saxon potential with the radius and diffuseness parameters fixed to 1.25 and 0.7 fm. The potential depths were adjusted to give the (known) eigenenergies for the initial states and specified low-energy scattering parameters (resonance energy or  $s$ -wave scattering length  $a_s$ ) for the continuum states [15]. In order to be able to compare with other experiments which cite “energies of resonances” [2], it is convenient to be able to translate a deduced  $a_s$  into an excitation energy scale. To this end we note that for bound states just below the threshold, the eigenenergy is approximately  $E = -\hbar^2/2ma_s^2$ . Consequently it seems logical to define the equivalent energy of the virtual state to be the same with opposite sign.

As in our previous experiments [2,3] it is necessary to consider the possible presence of a “background” contribution, by which we refer to reaction channels other than the one of interest. In the  $^{11}\text{Be}$  experiments there are two evident candidates for this. The first arises because the spectroscopic factor of the  $1s_{1/2}$  single-particle configuration is 0.74 [1] with a large part of the remainder representing a much more strongly bound  $0d_{5/2}$  state coupled to core excitations. Secondly, in the two experiments with  $^{11}\text{Be}$  the low binding of the halo neutron implies that the selection rule used for determining  $l$  is relaxed by the recoil momentum of the  $^9\text{Li}$  and  $^8\text{He}$  residues, of the order of 80 MeV/c in both cases. The transformation to the new center-of-mass system reduces this momentum by an order of magnitude, but it is still comparable to that of the halo. We estimate [15] by extending an analytical expression given by Bertsch *et al.* [16] that recoil reduces the intensity of the lowest components of the final  $l=0$  spectrum by approximately 10%, which will appear as a broader component.

We have approximated the background by folding the projected neutron and fragment velocity distributions from the coincidence data. These distributions are close to Gaussian shape and quite similar to the thermal distributions used in the previous work. They reflect mainly the limitations in experimental acceptance and differ little between the different projectile-product pairs. We have included such a shape in each fit and allowed the intensity to vary freely. The resulting intensity is 47% for ( $^{11}\text{Be}, ^9\text{Li}+n$ ) and 29% for ( $^{11}\text{Be}, ^8\text{He}+n$ ). A fit to the true coincident events requires a final-state interaction which gives rise to a narrower distribution than the intrinsic momentum distribution of the  $^{11}\text{Be}$  valency neutron, which for comparison is shown in Fig. 2b. We take this as proof that we are dealing with a real effect.

Figure 1(a) shows the velocity difference spectrum for the  $^6\text{He}+n$  system with the  $^{12}\text{Be}$  beam. As mentioned, the selection rule effect is not present here, and the reaction selects the peaks corresponding to forward- and backward-emitted neutrons from the  $0p_{3/2}$  resonance in  $^7\text{He}$ . This was previously observed in the  $^7\text{Li}(t, ^3\text{He})^7\text{He}$  reaction [17] at an energy of  $440 \pm 30$  keV and with a width of  $160 \pm 30$  keV. The fit to the data from the  $^{12}\text{Be}$  projectile (solid) is a sum of the model calculation with a resonance at 450 keV (short dashes) and the background (dot-dashed). A  $\chi^2$  analysis of this and similar results for  $^{11}\text{Be}$ , yielded an energy for the  $^7\text{He}$  state of  $450 \pm 20$  keV, in very good agreement with the previous measurement, and we present this as an independent determination. The error limits given here and in the following correspond to four units of increase in  $\chi^2$  from the best fit, indicating a significant change in the quality of the fit.

Figure 1(b) shows the corresponding spectrum for the  $^9\text{Li}+n$  system for the three different projectiles  $^{10,11,12}\text{Be}$ . The most striking qualitative result is the almost total absence of  $^9\text{Li}+n$  events from  $^{10}\text{Be}$ , which cannot give rise to

${}^9\text{Li}+n$  in a pure projectile fragmentation process. This proves that our technique, designed to observe projectile fragmentation, discriminates effectively against reaction products, including neutrons, originating in the target. The difference between the  ${}^{11}\text{Be}$  and the  ${}^{12}\text{Be}$  spectra also shows the influence of the initial state, the more bound  $s$  state in  ${}^{12}\text{Be}$  leading to a broader distribution.

Figure 2(a) shows  ${}^{10}\text{Li}$  data with the potential model fit for the  ${}^{11}\text{Be}$  projectiles. It confirms the strong final-state interaction at low energy observed in the previous work [2,3] using  ${}^{18}\text{O}$  as the projectile. The fact that we see this effect with  ${}^{11}\text{Be}$  proves that the state must have  $l=0$ , the same as the main single-particle contributor in the projectile. The scattering length is numerically very large, more negative than  $-20$  fm corresponding to an excitation energy of less than  $0.05$  MeV for the virtual state. The intensity of a  $p$  state assumed to be at  $0.5$  MeV in the final system is an unconstrained fit. As could be expected from the absence of a suitable initial state, the contribution is much smaller than it was with the  ${}^{18}\text{O}$  projectile [2,3], which has a full  $0p_{1/2}$  subshell.

For  ${}^9\text{He}$ , only the  ${}^{11}\text{Be}$  data had enough statistics to be of interest. The velocity distribution shown in Fig. 2(b) requires a final-state interaction characterized by a scattering length of the order of  $-10$  fm (or more negative), corresponding to an energy of the virtual state of  $0.0-0.2$  MeV. No combination of the background and the intrinsic momentum distribution of the  ${}^{11}\text{Be}$  valency neutron (corresponding to an  $s$ -wave scattering length  $a_s$  of zero) will fit the data. The selection rule again fixes the angular momentum to be zero. This suggests the level scheme shown in Fig. 3, in which the narrow resonances seen in previous work [6–8] are identified as excited levels about  $1.2$  MeV above threshold.

A theoretical spectrum for  ${}^9\text{He}$  calculated in a model space of  $[(0s)^4(0p)^n]$  ( $0\hbar\omega$ ) for negative parity states and  $[(0s)^3(0p)^{(n+1)}]$  plus  $[(0s)^4(0p)^{(n-1)}(0d1s)^{(1)}]$  ( $1\hbar\omega$ ) for positive parity states is shown for the WBP and WBT interactions of [18] in Fig. 3. The results we discuss for  ${}^{10}\text{Li}$  and  ${}^9\text{He}$  are predictions (extrapolations) based upon the  $0\hbar\omega$  and  $1\hbar\omega$  model and empirical Hamiltonians as described in Ref. [18]. If the configuration space for these nuclei is restricted to  $[(0p_{3/2})^4, 0p_{1/2}]$  and  $[(0p_{3/2})^4, 1s_{1/2}]$  for the  $1/2^-$  and  $1/2^+$  states, respectively, the  $1/2^+$  comes above the  $1/2^-$  state by  $2.38$  MeV. This restriction is equivalent to that assumed in a spherical Hartree-Fock calculation (with no pairing) and by three-body models for  ${}^{10}\text{He}$  ( ${}^{11}\text{Li}$ ) where  ${}^8\text{He}$  ( ${}^9\text{Li}$ ) are treated as inert (closed-shell) configurations. For the  $1/2^-$  state,  $(0p_{3/2})^4, 0p_{1/2}$  is the only configuration allowed in the  $p$ -shell. However for the  $1/2^+$  state the full  $p$ -shell space is represented by the three configurations  $[(0p_{3/2})^4, 1s_{1/2}]$ ,  $[(0p_{3/2})^2, (0p_{1/2})^2, 1s_{1/2}]$ , and  $[(0p_{3/2})^3, 0p_{1/2}, 1s_{1/2}]$ . The most important mixing is due to the pairing interaction between the first two of these, and this lowers the energy of the  $1/2^+$  state by  $3.32$  MeV and results in a crossing of the quasi-particle levels. This contribution is present in all  $N=7$  isotones and reaches a maximum of  $4.52$  MeV for  ${}^{11}\text{Be}$ .

The comparison presented in Fig. 3 suggests that the theoretical and experimental level spectra are in close agreement. However, the calculated neutron separation energy for the  $1/2^+$  ground state is  $-4.1$  MeV (unbound), in contrast to a value close to zero given by the present experiment. Similarly, the calculated neutron separation energy for the  $1/2^-$  state is  $-4.7$  MeV in contrast to the experimental value of  $-1.2$  MeV for the lowest resonance observed in the transfer reactions, which is suggested to be a  $p$  wave resonance due to its narrow shape. Thus the WBT (and WBP) extrapolations appear to be good for the spectrum but poor for the absolute energies with respect to  ${}^8\text{He}$ . This disagreement on the separation energy of the  $1/2^-$  state is common with other shell-model calculations [19,20] and might be due to other correlations and other states formed from the excitation of two or more particles from the  $p$  shell into the  $sd$  shell. However, the empirical WBT and WBP interactions are determined under the conditions that these higher excitations are not explicitly present in the low-lying states, and that their effect enters implicitly in terms of the effective one- and two-body matrix elements. Perhaps the close spacing of the  $p$  and  $s$  orbits near the neutron drip line makes the  $\hbar\omega$  restriction more unreliable than it appears to be in nuclei closer to stability.

In summary, our results strongly suggest for the first time, that the ground state of  ${}^9\text{He}$  is an unbound  $s$ -state with a scattering length of  $a_s \leq -10$  fm.  ${}^9\text{He}$  represents the lightest possible  $N=7$  nucleus. Based on this result, the mass assignment for  ${}^9\text{He}$  [21] has to be revised downward by 1 MeV. The appearance of intruder states as the ground states of  ${}^9\text{He}$  continues the trend observed in  ${}^{11}\text{Be}$  and  ${}^{10}\text{Li}$  and is in excellent agreement with the model [18] constructed for understanding the  $0p - 0d1s$  cross-shell interaction [22,23].

We acknowledge the help of T. Aumann, F. Deák, Á. Horváth, K. Ieki, Y. Iwata, Y. Higurashi, Á. Kiss, J. Kruse, V. Maddalena, H. Schelin, Z. Seres, and S. Takeuchi during the experiment, M. Steiner and J. Stetson for producing the radioactive beams, and P. Danielewicz for discussions. This work was supported by the National Science Foundation under grants PHY-9528844 and PHY-9605207.

## References

- [1] T. Aumann *et al.*, Phys. Rev. Lett. **84**, 35 (2000), and references therein.
- [2] M. Thoennessen *et al.*, Phys. Rev. C **59**, 111 (1999).
- [3] R.A. Kryger *et al.*, Phys. Rev. C **37**, R2439 (1993).
- [4] M. Zinser *et al.*, Phys. Rev. Lett. **75**, 1719 (1995).
- [5] M. Zinser *et al.*, Nucl. Phys. **A619**, 151 (1997).
- [6] K.K. Seth *et al.*, Phys. Rev. Lett. **58**, 1930 (1987).

- [7] H.G. Bohlen *et al.*, Z. Phys. A **330**, 227 (1988).
- [8] W. von Oertzen *et al.*, Nucl. Phys. **A588**, 129c (1995).
- [9] A.A. Ogloblin, Z. Phys. A **351**, 355 (1995).
- [10] K.M. Watson, Phys. Rev. **88**, 1163 (1952).
- [11] B.M. Sherrill *et al.*, Nucl. Instrum. Methods B **70**, 298 (1992).
- [12] J.J. Kruse *et al.*, to be published.
- [13] P.D. Zecher, *et al.*, Nucl. Instrum. Methods A **401**, 329 (1997).
- [14] L. Chen, Ph.D. Thesis, Michigan State University, March 2000.
- [15] L. Chen *et al.*, to be published.
- [16] G.F. Bertsch *et al.*, Phys. Rev. C **57**, 1366 (1998).
- [17] R.H. Stokes and P.G. Young, Phys. Rev. Lett **18**, 611 (1967); Phys. Rev. **178**, 2024 (1969).
- [18] E.K. Warburton and B.A. Brown, Phys. Rev. C **46**, 923 (1992).
- [19] N.A.F.M. Poppelier, L.D. Wood and P.W.M. Glaudemans, Phys. Lett. **157B**, 120 (1985).
- [20] S. Pieper, private communication.
- [21] G. Audi and A.H. Wapstra Nucl. Phys. **A595**, 409 (1995).
- [22] H. Sagawa, B.A. Brown and H. Esbensen, Phys. Lett. **B309**, 1 (1993).
- [23] B.A. Brown, in *International School of Heavy-Ion Physics, 4<sup>th</sup> Course: Exotic Nuclei*, ed. by R.A. Broglia and P.G. Hansen (World Scientific, Singapore, 1998) p1; *Proc. ENAM95*, ed. by M. de Saint Simon and O. Sorlin, Editions Frontieres (1995) p. 451.



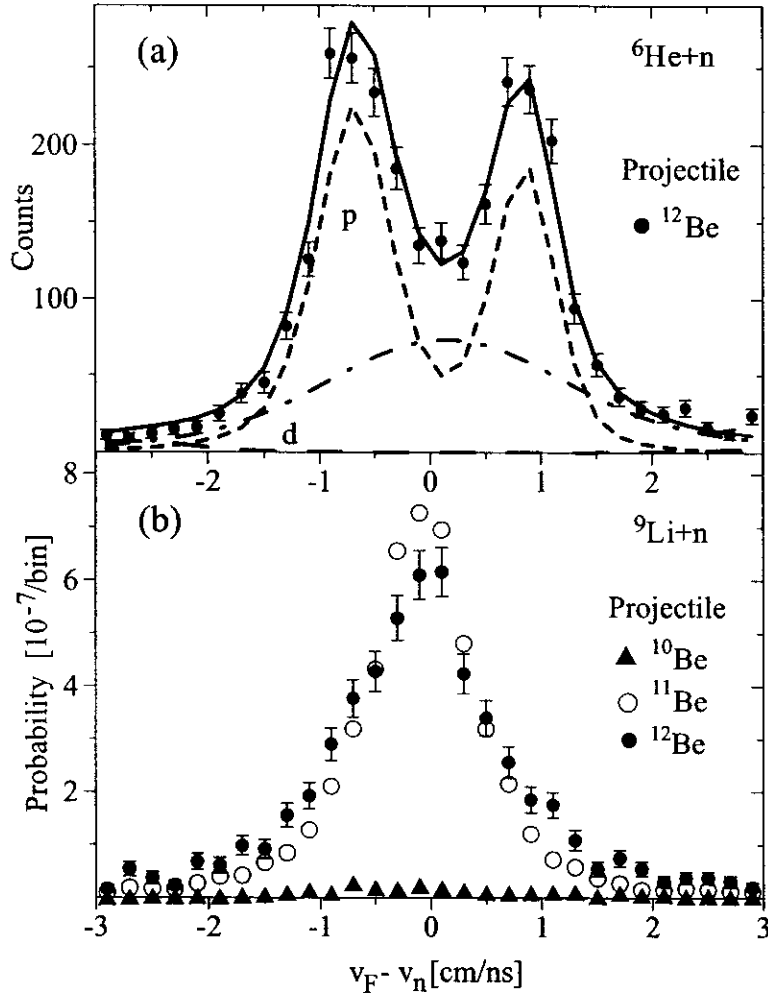


Fig. 1. Measured neutron-fragment velocity-difference spectra for  ${}^7\text{He}$  and  ${}^{10}\text{Li}$ . (a):  ${}^7\text{He}$  was produced in the reaction  ${}^9\text{Be}({}^{12}\text{Be}, {}^6\text{He}+n)\text{X}$  and the fit (solid) was adjusted to a  $p$ -wave resonance at  $450 \pm 20$  keV (short-dashed), a background contribution (dot-dashed) and a  $d$  component (long-dashed). (b): Three different projectiles  ${}^{10,11,12}\text{Be}$  producing  ${}^{10}\text{Li}$ . The intensity (shown in absolute units of  $10^{-7}$  per bin of 0.2 cm/ns) is normalized to the number of incoming fragments. Note the absence of events from the  ${}^{10}\text{Be}$  beam, which demonstrates the clean selection of events corresponding to decay of the projectile residue.

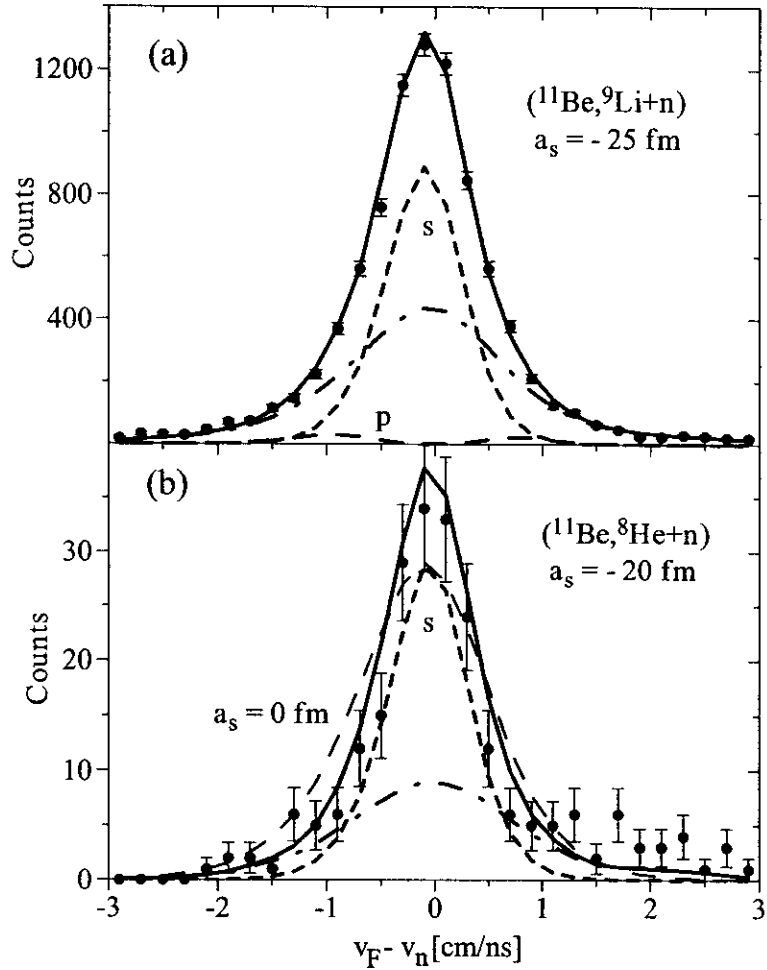


Fig. 2. Velocity difference spectra for the reactions of  $^{11}\text{Be}$  leading to  $^{10}\text{Li}$  (a) and  $^9\text{He}$  (b). The adjustment assumes  $s$ -wave components (short-dashed) characterized by a scattering length  $a_s = -25$  and  $-20$  fm, respectively, a background contribution (dot-dashed) and, for  $^{10}\text{Li}$ , a  $p$ -wave resonance at 0.50 MeV (long-dashed). The curve marked  $a_s = 0$  in (b) is the distribution calculated assuming no final-state interaction and without background contribution (long-dashed).

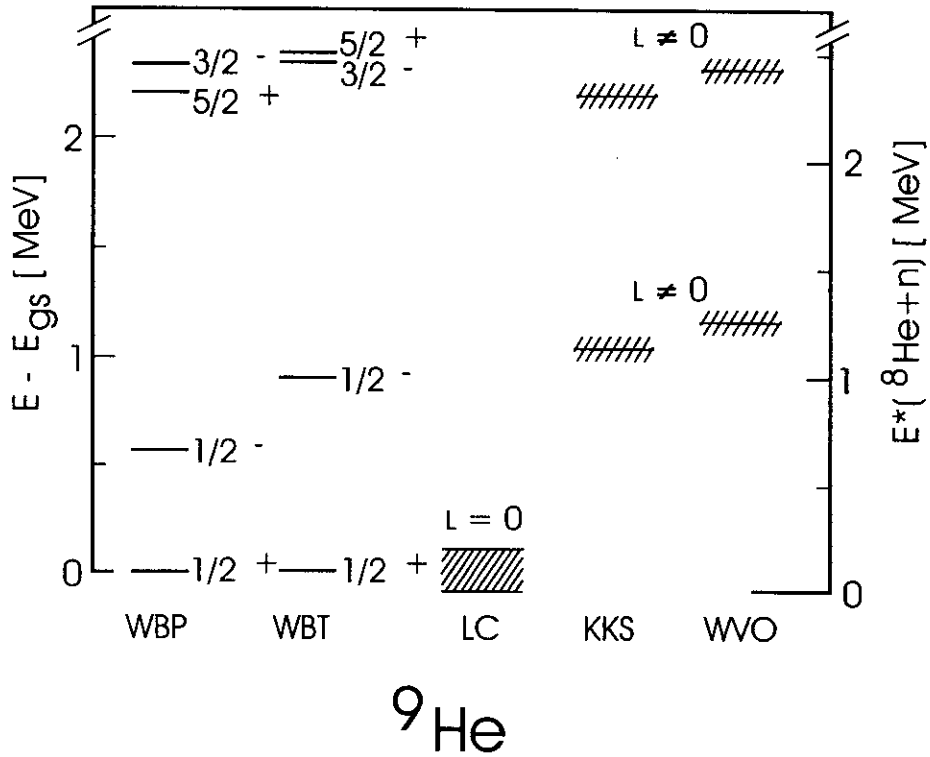


Fig. 3. Level scheme of  ${}^9\text{He}$ . Theoretical calculations with the WBP and WBT interactions of Warburton and Brown [18] are compared with the result of the present work (marked LC) and previously reported resonances in the  ${}^8\text{He}+n$  exit channel marked KKS [6] and WVO [7,8].